Appl Phys A (2010) 100: 1205–1209
DOI 10.1007/s00339-010-5838-2

Applied Physics A
Materials Science & Processing

Phase evolution, Raman spectroscopy and microwave dielectric behavior of ($Li_{1/4}Nb_{3/4}$) doped ZrO_2-TiO_2 system

Li-Xia Pang · Hong Wang · Di Zhou · Yue-Hua Chen · Xi Yao

Received: 2 November 2009 / Accepted: 10 May 2010 / Published online: 18 June 2010

Abstract The phase evolution, Raman spectroscopy and microwave dielectric properties of ($Li_{1/4}Nb_{3/4}$) doped ZrO_2-TiO_2 system were investigated. The effects of the Zr/Ti ratio and the ($Li_{1/4}Nb_{3/4}$) substitution were addressed. X-ray diffraction and electron diffraction analysis showed that the crystalline phases of the ($Li_{1/4}Nb_{3/4}$) doped ZrO_2-TiO_2 ceramics depended greatly on the Zr/Ti ratio. The sample with Zr/Ti ratio of 7/9 crystallized as $Zr_5Ti_7O_{24}$ phase structure, a commensurate structure with a tripled *a*-axis superstructure and a $Z^{TT}Z_{TT}$ sequence. Secondary phase of monoclinic ZrO_2 phase appeared when the Zr/Ti ratio was as high as 9/7. Raman analysis showed that the Raman peaks located at 651 and 624 cm^{-1} were assigned to the vibration modes of Zr-O octahedron and Ti-O octahedron, respectively. The dielectric constant and quality factor (*Qf* value) of the ($Li_{1/4}Nb_{3/4}$) doped ZrO_2-TiO_2 ceramics decreased slightly as the Zr/Ti ratio changed from 6/10 to 9/7. The temperature coefficient of resonate frequency (*TCF* value) was sensitive to the Zr/Ti ratio and it showed a negative value when the Zr/Ti ratio was close to 5:7. Meanwhile, the *TCF* value of ZrO_2-TiO_2 ceramics could also be tailored by the ($Li_{1/4}Nb_{3/4}$) substitution.

L.-X. Pang (✉) · H. Wang · D. Zhou · Y.-H. Chen · X. Yao
Electronic Materials Research Laboratory, Key Laboratory of the Ministry of Education, Xi'an Jiaotong University, Xi'an 710049, China
e-mail: l.x.pang@stu.xjtu.edu.cn
Fax: +86-298-3208210

L.-X. Pang
Laboratory of Thin Film Techniques and Optical Test, Xi'an Technological University, Xi'an 710032, China
e-mail: plx1982@gmail.com

1 Introduction

In recent years, ZrO_2-TiO_2 ceramics have attracted a great deal of interest due to their specific electrical and structural properties [1–4]. Because of their good microwave dielectric properties, the ZrO_2-TiO_2 ceramics are currently amongst the most widely used microwave dielectrics [5, 6]. In 1996, Azough et al. [7] discovered that the dielectric constant of zirconium titanate ceramic decreased as its cooling rate decreased to lower than 6°C/h, which was due to the phase transition during the cooling process. Thoitzsch et al. [8] studied the ZrO_2-TiO_2 phase diagram intensively and their work showed that there are two ordered phases with different compositions in ZrO_2-TiO_2 system. Between 1130 and 1080°C, the ZrO_2-TiO_2 near the composition $ZrTiO_4$ crystallizes as the 1:1 ordering phase [8] with two layers of distorted Zr sites plus two layers of octahedral Ti sites alternately stacking along the a-axis (called as 2× commensurate structure, Fig. 1(b)). At 1060°C and below, the ZrO_2-TiO_2 with composition near 5:7 displays another type of ordering phase [8], in which the Zr is hosted in one of every three cation layers (Zr site approaches eightfold coordination, named as 3× commensurate structure, Fig. 1(c) [9]). Usually, the $(Zr, Ti)_2O_4$ ceramics displays an α-PbO_2 orthorhombic structure with a random distribution of the Zr and Ti cations at equivalent octahedral sites (high-temperature disordered phase, Fig. 1(a) [9, 10]) at atmosphere pressure when temperatures exceed 1400°C, and it persists metastably at lower temperature because the ordering process is sluggish. However, when it is cooled at a very low cooling rate (e.g. 6°C/h), the structure will transform from the high-temperature disordered phase to 2× or 3× ordered structures (depending on the composition of the sample).

Nowadays, because of the development of low-temperature co-fired ceramic (LTCC) technology, many researchers

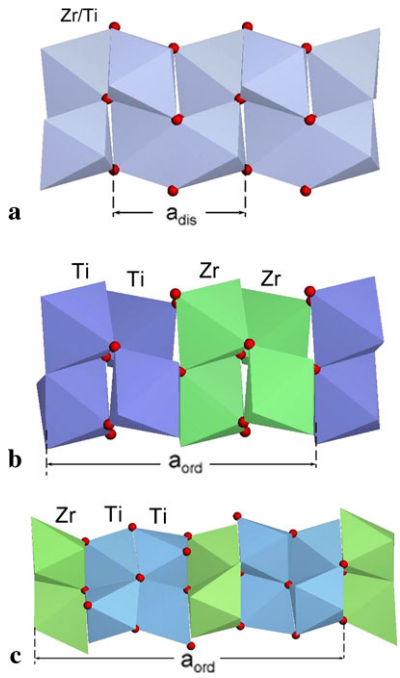

Fig. 1 [010] projection of zirconium titanate structures. Disordered zirconium titanate solid solution with the α–PbO_2 structure: (**a**) commensurate ordered structure (2×) for composition close to $ZrTiO_4$; (**b**) commensurate ordered structure (3×) for composition close to $Zr_5Ti_7O_{24}$ (**c**)

are trying to lower the sintering temperature of the zirconium titanate based ceramic [11–16]; however, it is very difficult to lower the sintering temperature to below 1300°C without serious deterioration in microwave dielectric properties. Our previous work [17] showed that $(Li_{1/4}Nb_{3/4})$ substitution was an effective way to lower the sintering temperature of $ZrTiO_4$ ceramic. The $Zr_{1-x}(Li_{1/4}Nb_{3/4})_xTiO_4$ ($x = 0.4$) ceramic which was sintered at 1170°C for 3 hrs showed good microwave dielectric properties with dielectric constant $(\varepsilon_r) = 41$, quality factor $(Qf) = 38000$ GHz and temperature coefficient of resonant frequency $(TCF) = 23.7$ ppm/°C. Since the microwave dielectric properties and phase structure of ZrO_2-TiO_2 ceramics are sensitive to the composition and sintering temperature [7, 8], it is necessary to study the evolution of the phase structure and the changes of microwave dielectric properties with the Zr/Ti ratio in the $(Li_{1/4}Nb_{3/4})$ doped ZrO_2-TiO_2 system. In this work, $(Li_{1/4}Nb_{3/4})_{0.4}Zr_xTi_yO_4$ ($x + y + 0.4 = 2$, $x/y = 7/9, 8/8, 9/7$) ceramics were prepared by conventional solid state reaction method to study the influence of the Zr/Ti ratio on the phase evolution, phonon vibrations and microwave dielectric properties in the $(Li_{1/4}Nb_{3/4})$ doped ZrO_2-TiO_2 system.

2 Experimental procedure

The $(Li_{1/4}Nb_{3/4})_{0.4}Zr_xTi_yO_4$ ($x + y + 0.4 = 2$, $x/y = 7/9, 8/8, 9/7$, marked as Z7T9, Z8T8 and Z9T7) specimens were prepared by the conventional solid state reaction method using high-purity reagent-grade raw materials of Li_2CO_3 (>99%, Guo-Yao Co. Ltd., Shanghai, China), Nb_2O_5 (>99%, Zhu-Zhou Harden Alloys Co. Ltd., Zhuzhou, China), rutile TiO_2 (>99%, Linghua Co. Ltd., Zhaoqing, China) and ZrO_2 (>99.5%, Xinxing Co. Ltd., Yixing, China). The raw materials were weighted and ball milled for 4.5 hrs. The mixtures were calcined at 950∼1000°C for 5 hrs and then re-milled for 5 hrs. The re-milled powders were dried and granulated with Polyvinyl Alcohol (PVA) binder and pressed into cylinders (10 mm in diameter and 5 mm in height) in a steel die under uniaxial pressure of 200 MPa. The cylinders were sintered in air at 1080∼1300°C for 3 hrs.

The crystalline phases of the samples were investigated by X-Ray diffraction (XRD) using an X-ray diffractometry with CuKα radiation (Rigaku D/MAX-2400 X-ray diffractometry, Tokyo, Japan) and electronic diffraction (ED) using an transmission electron microscope (JEM-3010, JEOL, Tokyo, Japan). The microstructures of the fracture surfaces were observed by scanning electron microscopy (SEM) (JSM-6360LV, JEOL, Tokyo, Japan) coupled with energy-dispersive X-ray spectroscopy (EDS).

Raman spectra were obtained using a Raman spectrometer (ALMEGA 1110, Nicolet, Wisconsin, Madison, USA), equipped with a diffraction grating of 2400 lines/mm, a spectrograph aperture with a 25 μm slit. The microscope attachment was an Olympus BX50 system and the excitation wavelength used was 532 nm from a Nd:YVO4 laser source.

The dielectric behaviors at microwave frequency of the samples were measured by the $TE_{01\delta}$ shielded cavity method [18] using a network analyzer (8720ES, Agilent, Palo Alto, CA, USA) and a temperature chamber (DELTA 9023, Delta Design, Poway, CA, USA). The quality factor was characterized by Qf ($Q \times f$, $Q = 1$/dielectric loss, f = resonant frequency) value. The TCF value was calculated by the following formula:

$$TCF = \frac{f_{85} - f_{25}}{f_{25} \times (85 - 25)} \quad (1)$$

where f_{85} and f_{25} were the $TE_{01\delta}$ resonant frequencies at 85 and 25°C, respectively.

3 Results and discussion

Figure 2(a) illustrates the XRD patterns of the well-densified $(Li_{1/4}Nb_{3/4})_{0.4}Zr_xTi_yO_4$ ceramics sintered at the same sintering temperature. The Z8T8 ceramic presents the high-temperature $ZrTiO_4$ crystalline phase (JCPDS file number

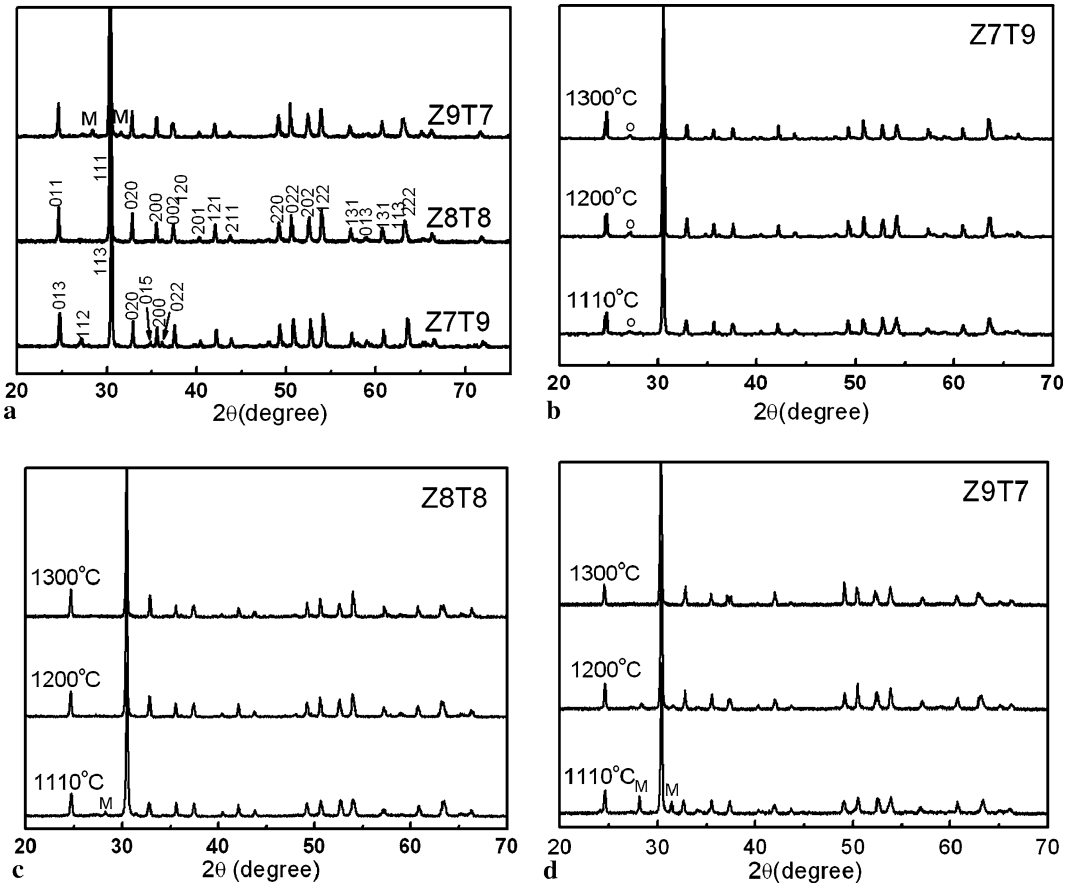

Fig. 2 XRD patterns for powders of Z7T9, Z8T8 and Z9T7 ceramics sintered at 1200°C (**a**), Z7T9 (**b**), Z8T8 (**c**) and Z9T7 (**d**) sintered at 1110, 1200 and 1300°C (M: monoclinic ZrO_2 phase, O: superlattice diffraction)

34-415), and the sample with Zr/Ti ratio of 7/9 shows the 3× commensurate ordered structure. The superstructural reflections of 5:7 ordering are detected in the XRD pattern of Z7T9 ceramic. When the Zr/Ti ratio is as high as 9/7, monoclinic ZrO_2 phase appears as the secondary phase. The XRD patterns of samples sintered at various temperatures were also measured to study the phase evolution of ($Li_{1/4}Nb_{3/4}$) doped ZrO_2-TiO_2 system. As shown in Fig. 2(b), the Z7T9 sample shows single 3× commensurate ordered phase structure through the whole sintering temperature range, while in Z8T8 sample, there are still a small amount of residual monoclinic zirconium oxides when sintered at 1110°C. As shown in Fig. 2(d), the content of secondary phase of monoclinic ZrO_2 in the Z9T7 ceramic decreases greatly with the sintering temperature and disappears when the sintering temperature is as high as 1300°C. It indicates that the solid solution range of the high-temperature $ZrTiO_4$ phase enlarged with the temperature, which agrees with the result reported by Azough et al. [7].

The Raman spectra of ($Li_{1/4}Nb_{3/4}$) doped ZrO_2-TiO_2 ceramics were measured to study the influence of ($Li_{1/4}Nb_{3/4}$) substitution and Zr/Ti ratio on the vibration

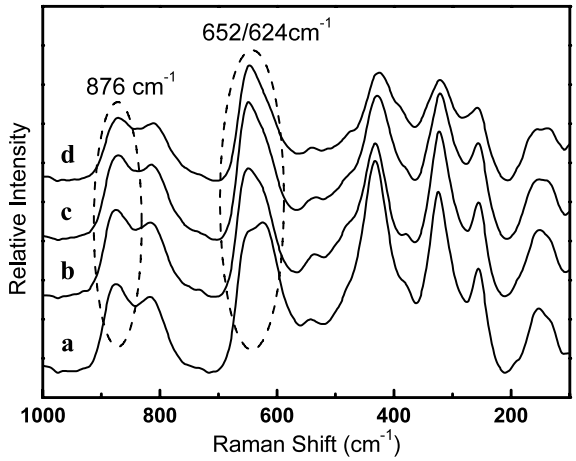

Fig. 3 Raman spectroscopy of Z6T10 (**a**), Z7T9 (**b**), Z8T8 (**c**) and Z9T7 (**d**) ceramics sintered at 1200°C for 3 hrs

modes. Figure 3 shows the room-temperature Raman spectra of $(Li_{1/4}Nb_{3/4})_{0.4}Zr_xTi_yO_4$ ceramics in the frequency range 100–1000 cm^{-1}. As shown in Fig. 3, when $x \leq 0.8$ the Raman modes at 255, 324, 432, 540, 813 and 876 cm^{-1} changed little with the Zr/Ti ratio increasing. The relative

intensities of Raman peaks located at 651 and 624 cm^{-1} change distinctly when the Zr/Ti ratio increases from 6/10 to 8/8, and these two Raman peaks amalgamate with each other as the ratio of Zr/Ti increases further. It indicates that the Raman peaks located at 651 and 624 cm^{-1} are assigned to the vibration modes of Zr-O octahedron and Ti-O octahedron respectively. With the Zr/Ti ratio increasing from 6/10 to 8/8, the phase structure of the $(Li_{1/4}Nb_{3/4})$ doped ZrO_2-TiO_2 ceramic transited from the 3× commensurate ordered phase to the high-temperature disordered $ZrTiO_4$ phase. As a consequence, the Zr-O/Ti-O octahedron ordering was weakened, which was responsible for the amalgamation of Raman modes located at 651 and 624 cm^{-1}. When the Zr/Ti ratio was as high as 9/7, all the Raman bands were broadened distinctly because of the influence of the secondary phase. The Raman-active mode at 876 cm^{-1} was an extra Raman-active mode in $(Li_{1/4}Nb_{3/4})$ doped ZrO_2-TiO_2 ceramics [17] and changed little with the Zr/Ti ratio. It suggests that the Raman-active mode centered at 876 cm^{-1} was not related to the Zr/Ti ratio but to the $(Li_{1/4}Nb_{3/4})$ substitution.

Usually, the appearance of new Raman-active modes reflects long-range or short-range cation ordering [19]. In complex perovskites, short-range cation ordering is apt to occur when the B sites are occupied by two or more types of cations with different electrovalences [19]. Whether a Li/Nb ordering happened in the $(Li_{1/4}Nb_{3/4})$ doped ZrO_2-TiO_2 system and whether the extra Raman-active mode at 876 cm^{-1} was caused by Li/Nb ordering were studied by electronic diffraction (ED) analysis, for ED analysis is a good method to study the cations ordering. Figure 4(a, b) corresponds to the [011] reciprocal lattice projections of Z8T8 ceramic and Z7T9 ceramic sintered at 1200°C. It is seen that the satellites in the electron microscopy pattern of Z8T8 specimen can be indexed as the disordered α-PbO_2-type diffraction. There is no new superlattice reflection except 100 and 011, which should disappear according to the extinction rule. In the electron microscopy of Z7T9, a 3-fold superstructure along a-axis is clearly visible, which is related to the 3× commensurate 5:7 superstructure, as illustrated in Fig. 4(c) [20]. The reflection satellites of 100 and 011 also appear in the Z7T9 specimen. However, because of the influence of double diffraction, it is difficult to determine whether the appearance of 100 and 011 reflection satellites corresponds to the $(Li_{1/4}Nb_{3/4})$ substitution or not. From the ED analysis, it is sure that the 1:3 Li/Nb short-range ordering does not occur in the $(Li_{1/4}Nb_{3/4})$ doped ZrO_2-TiO_2 system. The extra Raman-active mode at 876 cm^{-1} may be related with something else. Phonon calculation works on $Zr_5Ti_7O_{24}$ showed that there was a phonon vibration mode at 860 cm^{-1}, but it was Raman-silence. The $(Li_{1/4}Nb_{3/4})$ substitution in ZrO_2-TiO_2 system might have changed the phonon vibration mode centered at about 860 cm^{-1} from Raman-silence to Raman-active.

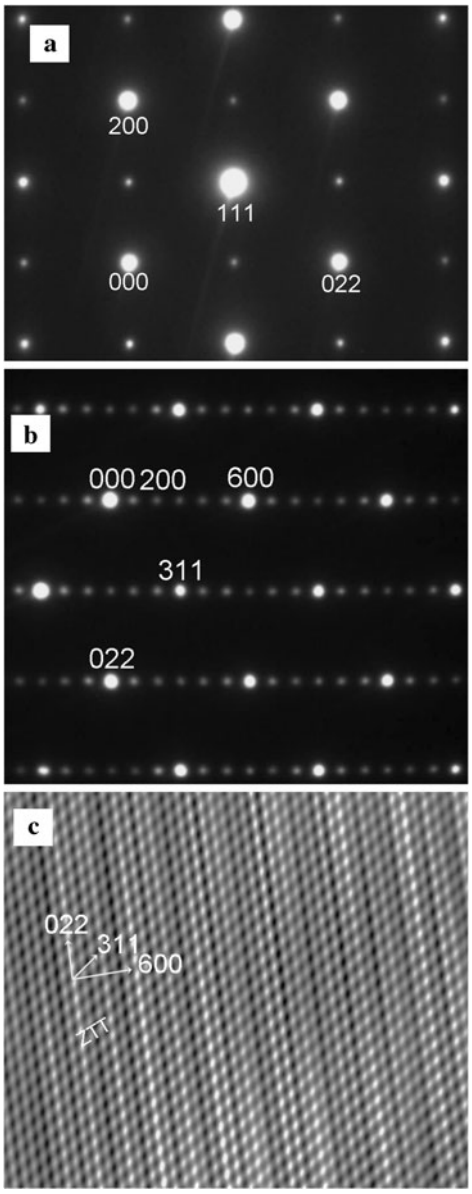

Fig. 4 [01$\bar{1}$] electron diffraction patterns for Z8T8 (**a**), Z7T9 (**b**) ceramics and [0$\bar{1}$1] high-resolution image of Z7T9 ceramic (**c**)

The Microwave dielectric properties (dielectric constant, *Qf* value and *TCF* value) of the $(Li_{1/4}Nb_{3/4})$ doped ZrO_2-TiO_2 ceramics as a function of Zr/Ti ratio are shown in Fig. 5. The dielectric constant ε_r decreased continually from 41.2 to 35.7 and the *Qf* value fell slightly from 38000 to 27000 GHz as the Zr/Ti ratio changed from 6/10 to 9/7. In the solid solution region, the microwave dielectric properties of $(Li_{1/4}Nb_{3/4})$ doped ZrO_2-TiO_2 ceramics depended greatly on the phase structure. In the rutile TiO_2 phase structure with $\varepsilon_r \sim 105$ [21], the Ti-O octahedral share edges with each other, and the essential contribution to the high ε_r stem from the hybridization of the oxygen p states with the *d* states of the Ti ions [1]. In the $ZrTiO_4$ composite, contiguous octahedral mostly share corners. Starting at Z8T8, more

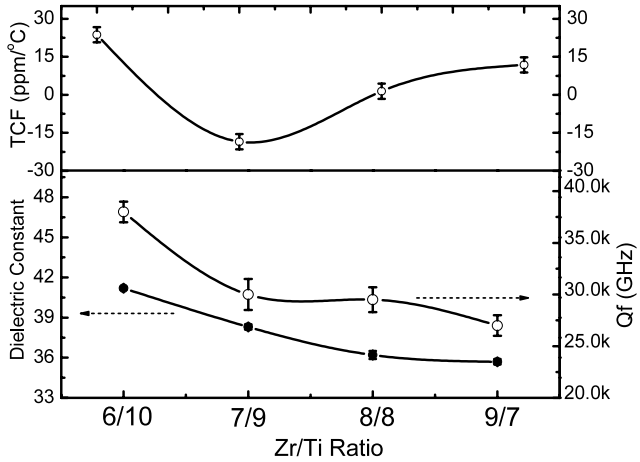

Fig. 5 Microwave dielectric properties (dielectric constant, *Qf* value and *TCF* value) of ($Li_{1/4}Nb_{3/4}$) doped ZrO_2-TiO_2 ceramics versus Zr/Ti ratio

octahedral share edges with the Ti content increasing, which result in the increase of the ε_r value. The *TCF* value shifted from +23.7 to −18.5 ppm/°C as the Zr/Ti ratio increased from 6/10 to 7/9, and then it shifted towards positive as the Zr/Ti ratio increased further. It indicates that the *TCF* value was sensitive to the Zr/Ti ratio in the ($Li_{1/4}Nb_{3/4}$) doped ZrO_2-TiO_2 system. When the Zr/Ti ratio was close to 5:7, the $(Li_{1/4}Nb_{3/4})_{0.4}Zr_xTi_yO_4$ ceramic showed a negative *TCF* value. Similar result was also given in our previous work [17]. Meanwhile, comparing with $ZrTiO_4$ having a *TCF* value of +64 ppm/°C [1], the ($Li_{1/4}Nb_{3/4}$) doped Z8T8 ceramic showed a *TCF* value of +1.4 ppm/°C. It means that the *TCF* value of ZrO_2-TiO_2 ceramics could also be tailored by the ($Li_{1/4}Nb_{3/4}$) substitution.

4 Conclusions

The influence of the Zr/Ti ratio and ($Li_{1/4}Nb_{3/4}$) substitution on the phase structure, phonon vibration and microwave dielectric properties in ($Li_{1/4}Nb_{3/4}$) doped ZrO_2-TiO_2 system were studied by XRD, TEM, Raman spectroscopy and microwave dielectric characterization. The Z8T8 ceramic presents the high-temperature $ZrTiO_4$ crystalline phase, and the sample with Zr/Ti ratio of 7/9 shows the 3× commensurate ordered structure. Raman analysis showed that the Raman peaks located at 651 and 624 cm^{-1} are assigned to the vibration modes of Zr-O octahedron and Ti-O octahedron respectively. The dielectric constant and quality factor (*Qf* value) of the ($Li_{1/4}Nb_{3/4}$) doped ZrO_2-TiO_2 ceramics decreased slightly as the Zr/Ti ratio changed from 6/10 to 9/7. The temperature coefficient of resonate frequency (*TCF* value) was sensitive to the Zr/Ti ratio and it showed a negative *TCF* value when the Zr/Ti ratio was close to 5:7. Meanwhile, the *TCF* value of ZrO_2-TiO_2 ceramics could also be adjusted by the ($Li_{1/4}Nb_{3/4}$) substitution. Z8T8 ceramic sintered at 1170°C showed good microwave dielectric properties of $\varepsilon_r = 36.2$, $Qf = 29500$ GHz and $TCF = +1.4$ ppm/°C.

Acknowledgements This work was supported by the National 973-project of China (2009CB623302), National Project of International Science and Technology Collaboration (2009DFA51820) and NSFC projects of China (60871044, 50835007).

References

1. G. Wolfram, E. Gőbel, Mater. Res. Bull. **16**, 1455 (1981)
2. S.X. Zhang, J.B. Li, J. Cao, H.Z. Zhai, B. Zhang, J. Mater. Sci. Lett. **20**, 1409 (2001)
3. Y.K. Kim, H.M. Jang, J. Appl. Phys. **89**, 6349 (2001)
4. J. Macan, A. Gajović, H. Ivanković, J. Eur. Ceram. Soc. **29**, 691 (2009)
5. Y. Park, Y.H. Kim, H.G. Kim, Mater. Sci. Eng. B **40**, 37 (1996)
6. A. Bianco, G. Gusmano, R. Freer, P. Smith, J. Eur. Ceram. Soc. **19**, 959 (1999)
7. F. Azough, R. Freer, C.L. Wang, G.W. Lorimer, J. Mater. Sci. **31**, 2539 (1996)
8. U. Troitzsch, D.J. Ellis, J. Mater. Sci. **40**, 4571 (2005)
9. P. Bordet, A. McHale, A. Santoro, R.S. Roth, J. Solid State Chem. **64**, 30 (1986)
10. R.E. Newnham, J. Am. Ceram. Soc. **50**, 216 (1967)
11. C.L. Huang, C.S. Hsu, R.J. Lin, Mater. Res. Bull. **36**, 1985 (2001)
12. D. Houivet, J.E. Fallah, J.M. Haussonne, J. Eur. Ceram. Soc. **19**, 1095 (1999)
13. W.S. Kim, J.H. Kim, J.H. Kim, K.H. Hur, J.Y. Lee, Mater. Chem. Phys. **79**, 204 (2003)
14. S.N. Koc, J. Sol-Gel Sci. Technol. **38**, 277 (2006)
15. J.H. Jean, S.C. Lin, J. Am. Ceram. Soc. **83**, 1417 (2000)
16. V.L. Arantes, D.P.F. de Souza, Mater. Sci. Eng. A **398**, 220 (2005)
17. L.X. Pang, H. Wang, D. Zhou, X. Yao, Jpn. J. Appl. Phys. **48**, 051403 (2009)
18. J. Krupka, K. Derzakowski, B. Riddle, J. Baker-Jarvis, Meas. Sci. Technol. **9**, 1751 (1998)
19. H. Zheng, H. Bagshaw, G.D.C. Csete de Győrgyfalva, I.M. Reaney, J. Appl. Phys. **94**, 2948 (2003)
20. R. Christoffersen, P.K. Davies, J. Am. Ceram. Soc. **75**, 563 (1992)
21. K. Fukuda, R. Kitoh, I. Awai, Jpn. J. Appl. Phys. **32**, 4584 (1993)